Enhancing Efficiency of Non-aqueous Li-CO_2 Battery with Molybdenum Disulfide as Cathode Catalyst by Highly Exposing Mo-edges

Chih-Jung Chen (陳致融)[1], Chih-Sheng Huang (黃志盛)[1], Yu-Cheng Huang (黃裕呈)[2], Chung-Li Dong (董崇禮)[2]*, and Ru-Shi Liu (劉如熹)[1]*

[1]Department of Chemistry, National Taiwan University, Taipei 10617, Taiwan
[2]Department of Physics, Tamkang University, Tamsui 25137, Taiwan

cldong@mail.tku.edu.tw; rsliu@ntu.edu.tw

Abstract

Intensive efforts have been devoted for developing Li-CO_2 batteries, because the potential application as the power supply of rovers for the outer space exploration. Besides, exploiting the electrochemical mechanisms behind Li-CO_2 cells assists to design the practical usage of Li-air batteries in an ambient atmosphere. Herein, molybdenum disulfide anchored on carbon nanotube (MoS_2/CNT) were synthesized as cathode for non-aqueous Li-CO_2 batteries. The optimal discharge capacity and coulombic efficiency of MoS_2/CNT cathode were 8551 mAh g^{-1} and 96.7%, respectively, achieved by exposing the highest amounts of Mo-edges.

Keywords - non-aqueous Li-CO_2 battery, cathode catalyst, molybdenum disulfide, Mo-edges

Introduction

Recently, lithium-air (Li-air) batteries have aroused significant attention owing to their extremely high theoretical energy density (ca. 3500 Wh kg^{-1}), which are highly desirable for long-mileage electric vehicles.[1] Among various systems of Li-air cells, National Aeronautics and Space Administration (NASA) has considerable interest in Li-CO_2 batteries, which are capable of being utilized as the power supplies of rovers for exploring alien planets, such as Mars that is full of CO_2 (ca. 96%) in its atmosphere.[1c, 2] Besides, resolving the electrochemical mechanisms of Li-CO_2 cells provides valuable insight for advancing Li-air batteries to be operated under ambient air.[3]

The working principle of a rechargeable Li-CO_2 batteries was based on driving electrochemical reactions as follow:

$$Li^+ + CO_2 + e^- \leftrightharpoons Li_2CO_3 + C$$

However, the Li_2CO_3 discharging product is a wide-band gap insulator with highly thermodynamic stability ($\Delta_f G^o$ = –1132.1 kJ mol^{-1}),[1c] leading to sluggish kinetics of CO_2 evolution reaction in the charging process. Furthermore, Li_2CO_3 residues gradually accumulated on the active sites of cathode upon cycling, and increased the charge transfer impedance of the cell. This result causes high overpotential, poor cycling performance, and limited rate capability of Li-CO_2 batteries.[4] Herein, molybdenum disulfide anchored on carbon nanotube (MoS_2/CNT) were synthesized as cathode for reversibly generating and decomposing Li_2CO_3 upon cycling measurements.

Experiments

CNT was mixed with various amounts of $(NH_4)_2MoS_4$, and subsequently dispersed in methanol as the precursor solutions for preparing of MoS_2/CNT materials. The precursor solution was stirred at room temperature until the mathanol solvent evaporated. The residual powder was then ground by a mortor, and placed in a alumina crucible for a thermolysis reaction in a tube furnance. After natually cooling down to room tempearature, MoS_2/CNT catalysts were sucessfully synthesized.

Results

In the present work, MoS_2 anchored on CNT as the catalyst cathode for non-aqueous Li-CO_2 battery. For convenience, we abbreviate CNT with different MoS_2 decorating amounts as "MoS_2/CNT-X," in which X represents MoS_2/CNT molar ratios. MoS_2/CNT-1 presented a discharge capacity of 2949 mAh g^{-1}, as shown in Figure 1a. Nevertheless, MoS_2/CNT-1 material barely delivered a moderate coulombic efficiency of 73.6% and large overpotential of 1.57 V. The electrochemical performance of MoS_2/CNT-X materials was optimized by MoS_2/CNT-3 catalyst. Its discharge capacity was theatrically enhanced to 8551 mAh g^{-1}, and coulombic efficiency was increased to 96.7%. The overpotential of MoS_2/CNT-3 was optimally improved to 1.24 V. However, further increasing MoS_2/CNT molar ratios, MoS_2/CNT-4 showed a reduced catalytic activity compared with MoS_2/CNT-3, as shown in Figure 1a. MoS_2/CNT-4 presented poorer discharge capacity and coulombic efficiency, that is, 6301 mAh g^{-1} and 91.7%, respectively.

Figure 1b shows Raman spectra of MoS_2/CNT and bare MoS_2 catalysts collected in air ambient environment. The vibration directions of E^1_{2g} and A_{1g} Raman modes are within the basal plane and along the c-axis, respectively. Hence, the area ratios (E^1_{2g} / E^1_{2g} + A_{1g}), calculated by integrating the Raman peak intensity, were adopted to analyze the texture information of MoS_2 materials. The E^1_{2g} and A_{1g} Raman modes are preferentially excited for terrace- and edge-terminated structures in MoS_2 catalysts, leading to high and low values of this area ratios, respectively.[5] In short, higher number of exposed edges of MoS_2 caused a lower area ratio. The increment of these area ratios followed the order of MoS_2/CNT-1 > MoS_2/CNT-2 > MoS_2/CNT-4 > MoS_2/CNT-3, which

correlates to the full discharging capacity and overpotential. This results demonstrates that exposed edges of MoS_2 catalysts functioned as the active sites for providing capacity and reducing overpotential. The electrochemical performance of Li-CO_2 cells was depended on the number of exposed edges on MoS_2 structure.

X-ray absorption spectroscopy (XAS) was applied to investigate the electronic and atomic structures of MoS_2/CNT catalysts. The oxidation states and local correlations of MoS_2/CNT materials were probed by using X-ray absorption near edge structure (XANES) and extended X-ray absorption fine structure (EXAFS), respectively. Mo foil was used as a Mo zero-valent standard, while MoO_3 commercial powder functioned as a standard of Mo^{6+} cation (Figure 1c). The energy of absorption edge is proportional to the oxidation states of samples given that highly valent cations show strong binding energy of core-level electrons, contributing to a chemical shift of X-ray absorption to the increased energy. All MoS_2/CNT catalysts showed a consistent Mo K-edge absorption energy which located between Mo foil and MoO_3 standards. This result indicates that Mo cations in MoS_2/CNT materials were +4 valence states. Radial distribution for Fourier transform Mo K-edge k^2-weighted EXAFS signal of MoS_2/CNT materials were revealed in Figure 1d. Two peaks were observed at approximately 1.9 and 2.8 Å, corresponding to Mo–S and Mo–Mo coordination shells, respectively. For Mo atoms on the basal plane, N_S and N_{Mo} are both 6. On the other hand, Mo atoms on Mo-edge are surrounded by 4 S and 4 Mo atoms in the first and second shell, whereas those on sulphur terminated Mo-edge (ST-Mo-edge) and S-edge are incorporated with the closest neighbors of 6 S and 4 Mo. The coordination number ratios (N_S/N_{Mo}) of basal plane and Mo-edge are equal to 1, while those of ST-Mo-edge and S-edge is 1.5. EXAFS fitting was adopted to acquire N_S/N_{Mo} values of MoS_2/CNT materials. The N_S/N_{Mo} ratios elevated with increasing the decorating amounts of MoS_2 on CNT. A higher coordination number ratio was possibly caused by high quantities of either exposed S-edge or ST-Mo-edge. Our theoretical DFT calculations presented that ST-Mo-edge on MoS_2 structure showed the ideal adsorption energy of Li, CO_2, and Li_2CO_3. Moreover, Raman spectra demonstrates that the highest amounts of edges existed in the MoS_2/CNT-3 catalyst, as compared with other composite materials. Thus, MoS_2/CNT-3 cathode exhibited a high N_S/N_{Mo} ratio and the optimal electrochemical efficiency, due to highly exposed ST-Mo-edge instead of S-edge.

Discussion

In summary, we developed MoS_2/CNT cathode catalysts for Li-CO_2 battery. XANES spectra revealed that Mo cations in MoS_2/CNT materials were +4 valence states. EXAFS result showed that MoS_2/CNT-3 presented the lowest N_S/N_{Mo} ratio of about 1.24, which exposed the highest amounts of Mo-edges. This result caused the optimal electrochemical performance of MoS_2/CNT-3 material.

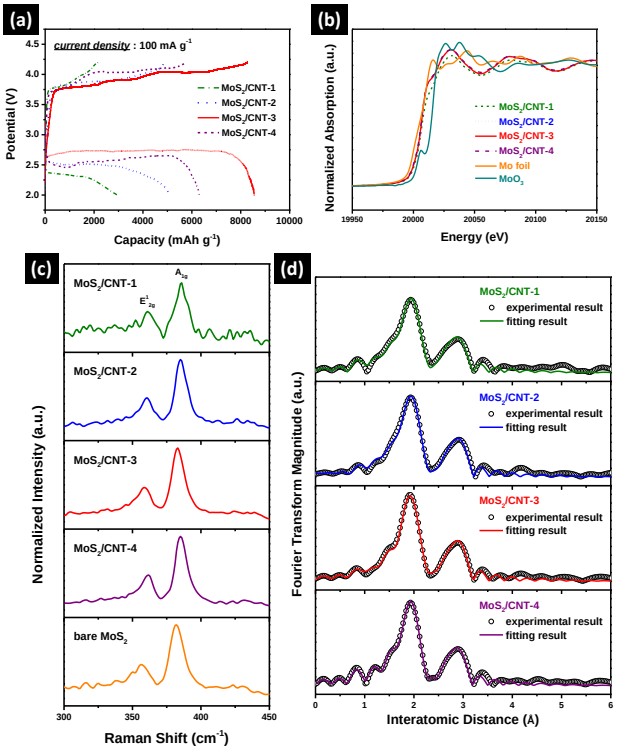

Figure 1. (a) Full discharge-charge profiles of MoS_2/CNT cathodes at a current density of 100 mA g^{-1} within a voltage window of 2.0~4.2 V. (b) Raman spectra of MoS_2/CNT and bare MoS_2 catalysts. Mo K-edge (c) XANES spectra and (d) radial distribution for Fourier transform k^2-weighted EXAFS signal of MoS_2/CNT materials.

Acknowledgment

The authors are grateful for the financial support from the Ministry of Science and Technology (Contract No. MOST 107-2113-M-002-008-MY3).

References

[1] a) P. G. Bruce, S. A. Freunberger, L. J. Hardwick, J.-M. Tarascon, *Nat. Mater.* **2011**, *11*, 19; b) J. Lu, Y. Jung Lee, X. Luo, K. Chun Lau, M. Asadi, H.-H. Wang, S. Brombosz, J. Wen, D. Zhai, Z. Chen, D. J. Miller, Y. Sub Jeong, J.-B. Park, Z. Zak Fang, B. Kumar, A. Salehi-Khojin, Y.-K. Sun, L. A. Curtiss, K. Amine, *Nature* **2016**, *529*, 377; c) L. Qie, Y. Lin, J. W. Connell, J. Xu, L. Dai, *Angew. Chem. Int. Ed.* **2017**, *56*, 6970-6974.

[2] a) Y. Hou, J. Wang, L. Liu, Y. Liu, S. Chou, D. Shi, H. Liu, Y. Wu, W. Zhang, J. Chen, *Adv. Funct. Mater.* **2017**, *27*, 1700564; b) X. Zhang, C. Wang, H. Li, X.-G. Wang, Y.-N. Chen, Z. Xie, Z. Zhou, *J. Mater. Chem. A* **2018**, *6*, 2792-2796.

[3] S. R. Gowda, A. Brunet, G. M. Wallraff, B. D. McCloskey, *J. Phys. Chem. Lett.* **2013**, *4*, 276-279.

[4] C. Ling, R. Zhang, K. Takechi, F. Mizuno, *J. Phys. Chem. C* **2014**, *118*, 26591-26598.

[5] a) D. Kong, H. Wang, J. J. Cha, M. Pasta, K. J. Koski, J. Yao, Y. Cui, *Nano Lett.* **2013**, *13*, 1341-1347; b) X. Dai, K. Du, Z. Li, M. Liu, Y. Ma, H. Sun, X. Zhang, Y. Yang, *ACS Appl. Mater. Interfaces* **2015**, *7*, 27242-27253.